

Slowly rotating black holes in the Einstein-Maxwell-scalar theory

Jianhui Qiu*

*National Astronomical Observatories, Chinese Academy of Sciences, Beijing 100101, China and
School of Astronomy and Space Sciences, University of Chinese Academy of Sciences,
No. 19A, Yuquan Road, Beijing 100049, China*

We make the research on a slowly rotating black hole solution in a new Einstein-Maxwell-scalar theory, which is an extension of the Einstein-Maxwell-dilaton theory. The gyromagnetic ratio of this black hole is calculated and it increases with the parameter β , but decreases with the parameter γ . In the Einstein-Maxwell-dilaton theory where the parameter β is in the absence, the gyromagnetic ratio is always less than 2, the gyromagnetic ratio for Kerr-Newman black hole. Now we find that the standard gyromagnetic ratio 2 can also be realized in this Einstein-Maxwell-scalar theory by increasing β and γ simultaneously. The same value of angular velocity of locally non-rotating observer as that in Kerr-Newman black hole can also be obtained in the same way. We also investigated the correction of period for circular orbits with respect to charge to mass ratio and the correction of radius of innermost stable circular orbits. We find that the correction becomes smaller and smaller with the increase of β . It is also shown that the radiative efficiency in the thin accretion disk model, for small value of β and large value of charge to mass ratio, the efficiency vanishes due to lacking of the enough stress and dynamic friction in the accretion model. A phantom Maxwell black hole is investigated in this theory as an example of exact slowly rotating black hole solution. Therefore, formula for angular velocity of the event horizon is shown. Correction of the radius of innermost stable circular orbits and of radiative efficiency are investigated subsequently. It is found that the correction up to first order of the perturbation parameter can vanish for some value of charge-to-mass ratio. The total radiative efficiency can also vanish once the effect of rotation is considered.

PACS numbers: 04.50.Kd, 04.70.Dy

I. INTRODUCTION

Despite the great success of Einstein's general gravity (GR) in continued consistency with observations, there are strong motivations for studying theories of gravity beyond GR which ranges from attempts for quantum theories of gravity [1], to explanation of phenomena including inflation [2, 3], dark matter [4] and dark energy [5, 6].

One of the first proposed theories in the literature, which is formulated in the Jordan frame, where the scalar-tensor theory is originally conceived, is the Brans-Dicke gravitational theory [7]. Brans-Dicke theory describes the gravity by the metric tensor and a scalar field non-minimally coupled to gravity, where the scalar field is identified as dilaton field by O'Hanlon [8], Acharia and Hogan [9]. Dilaton field which presents as a Nambu-Goldstone boson of broken scale invariance, might mediate a finite range gravity based on an idea in particle physics [10]. Indeed, by using of the conformal transformations, the action of Einstein-dilaton gravity theory is obtained from that of Jordan frame scalar-tensor theory. For a thorough understanding of scalar-tensor gravity and the relation to dilaton field, we refer the reader to the monograph by Fujii and Maeda [11].

As the low-energy limit of some underlying quantum theory of gravity, the dilaton field combined with axion field which is another field deduced from the low-energy limit of string theory, have achieved interesting consequences in inflationary cosmology and later time in the acceleration of the universe [12]. Exact static dilaton black hole solutions of Einstein-Maxwell-dilaton (EMd) gravity have been constructed by many authors [13–16]. However, exact rotating dilaton black hole solutions have been obtained only for some limited values of the dilaton coupling constant [17–20] among which the charged rotating Kerr-Sen solution which considers the dilaton field and axion field is the most famous

* jhqiu@nao.cas.cn

one. The Kerr-Sen solution in turn can provide an indirect test for string theory. Although the Kerr metric bears strong resemblance with the Kerr-Newman metric, the inherent geometry of the two black holes vary significantly. The distinguished properties of the two spacetimes have been extensively studied [21–23]. For general dilaton coupling constants, the properties of charged rotating dilaton black holes are studied only in the case of infinitesimal small charge [24] or small angular momentum [25–27]. Slowly Rotating solutions of the Einstein-Maxwell-Scalar black hole in asymptotically flat or AdS spacetime have been investigated extensively (for references see [28–30]).

Phantom field which is a special kind of dark energy model with the negative kinetic energy [31] has been applied extensively in cosmology to explain the acceleration of the Universe [32, 33]. Compared with the cosmological constant which is an essential ingredient of the Λ CDM model and the most popular dark energy model in Einstein gravity [34], the equation of state of the phantom field is less than -1 and the null energy condition is violated. But it is still not excluded by recent precise observational data [35]. The causal structures of black holes in the EMD theory when a phantom coupling is considered are studied completely by Clement [36].

Recently, by observing the Reissner Nordstrom solution, the Einstein-Maxwell-dilaton solution, the dilaton black holes in the anti-de Sitter universe in four dimensions [37] and arbitrary dimensions [38], we construct a new Einstein-Maxwell-Scalar theory in four dimensions [39] and arbitrary dimensions [40]. The coupling between scalar field and Maxwell field can be viewed as an extension of coupling between dilaton and Maxwell field. The coupling is indeed a combination of dilaton field with the Maxwell field with different coupling strength. The geodesics of this theory has been investigated in [41]. The present article is devoted to the study of the slowly rotating black hole in four dimensional and asymptotically flat spacetime. In this way, we hope to understand this theory further. The article is organized in the following way.

In Section II, we derive equations of motion for the slowly rotating black holes. In Section III, we explain the details of numerical solution to the black hole. In Section IV, we make a research on the case of normal coupling of scalar field and Maxwell field in two subsections, **A** and **B**. In subsection **A**, we study the angular momentum, angular velocity of the event horizon and the gyromagnetic ratio of the black hole. In subsection **B**, we compute the correction to geodesics due to the rotating effect. In Section V, we make an investigation on an exact slowly rotating phantom black hole solution of this theory and make an exploration on its angular velocity and correction to the particle motion. Finally, in Section VI, we make a discussion and summarize our results.

II. ACTION AND THE EQUATIONS OF MOTION

We start from the action of Einstein-Maxwell-scalar theory

$$S = \int d^n x \sqrt{-g} \left[R - \frac{4}{n-2} \nabla_\mu \phi \nabla^\mu \phi - V(\phi) - K(\phi) F^2 \right], \quad (1)$$

where R is the Ricci scalar curvature, $F^2 \equiv F_{\mu\nu} F^{\mu\nu}$ comes from the Maxwell field, $K(\phi)$ is the coupling function between scalar field and Maxwell field. $V(\phi)$ is the scalar potential. For the asymptotically dS or AdS solution, $V(\phi)$ is chosen as

$$V(\phi) = \frac{\lambda}{3(n-3+\alpha^2)^2} \left[-\alpha^2(n-2)(n^2-n\alpha^2-6n+\alpha^2+9) e^{\frac{4(n-3)\phi}{(n-2)\alpha}} + (n-2)(n-3)^2(n-1-\alpha^2) e^{-\frac{4\alpha\phi}{n-2}} + 4\alpha^2(n-3)(n-2)^2 e^{\frac{2\phi(n-3-\alpha^2)}{(n-2)\alpha}} \right], \quad (2)$$

and $K(\phi)$ is set as

$$K(\phi) = \frac{2(\alpha^2+n-3) e^{\frac{4\alpha\phi}{n-2}}}{2\alpha^2+(n-3)[2+(n^2-5n+6)\beta] + \beta\alpha^2(n-2)(n-3) e^{\frac{4(\alpha^2+n-3)\phi}{\alpha(n-2)}}}, \quad (3)$$

to achieve the solution in [40].

Varying the action with respect to the metric, Maxwell and the scalar field, respectively, yields

$$R_{\mu\nu} = \frac{4}{n-2} \nabla_\mu \phi \nabla_\nu \phi + \frac{V}{n-2} g_{\mu\nu} + 2K F_{\mu\alpha} F_\nu^\alpha - \frac{K}{n-2} F^2 g_{\mu\nu}, \quad (4)$$

$$\partial_\mu (\sqrt{-g} K F^{\mu\nu}) = 0, \quad (5)$$

$$\nabla_\mu \nabla^\mu \phi - \frac{n-2}{8} \left(\frac{\partial V}{\partial \phi} + \frac{\partial K}{\partial \phi} F^2 \right) = 0. \quad (6)$$

Then we will get a solution of static spherically symmetric spacetime

$$ds^2 = -U dt^2 + \frac{1}{U} \cdot \left[1 - \left(\frac{a}{r} \right)^{n-3} \right]^{-\gamma(n-4)} dr^2 + f^2 d\Omega_{n-2}^2, \quad (7)$$

with

$$U = \left[1 - \left(\frac{b}{r} \right)^{n-3} \right] \left[1 - \left(\frac{a}{r} \right)^{n-3} \right]^{1-\gamma(n-3)} - \frac{1}{3} \lambda r^2 \left[1 - \left(\frac{a}{r} \right)^{n-3} \right]^\gamma + \beta q^2 \left\{ r^2 \left[1 - \left(\frac{a}{r} \right)^{n-3} \right]^\gamma \right\}^{3-n}, \quad (8)$$

$$f = r \left[1 - \left(\frac{a}{r} \right)^{n-3} \right]^{\gamma/2}, \quad (9)$$

$$\gamma \equiv \frac{2\alpha^2}{(n-3)(n-3+\alpha^2)}, q^2 = \frac{(n-2)(n-3)^2}{2(n-3+\alpha^2)} a^{n-3} b^{n-3}. \quad (9)$$

The scalar field should be

$$\phi = -\frac{(n-2)\alpha}{2(\alpha^2+n-3)} \ln \left[1 - \left(\frac{a}{r} \right)^{n-3} \right]. \quad (10)$$

In this article, we restrict ourselves to the case of four dimensions and devote ourselves to finding a slowly rotating black hole solution in the asymptotically flat spacetime, i.e. $n = 4$ and $\lambda = 0$. Then the theory is given by

$$S = \int d^4x \sqrt{g} \left(R - 2\nabla_\mu \phi \nabla^\mu \phi - \frac{e^{-\frac{2\phi}{\alpha}} (\alpha^2 + 1)}{(\alpha^2 + \beta + 1) e^{-\frac{2\phi(\alpha^2+1)}{\alpha}} + \beta \alpha^2} F^2 \right), \quad (11)$$

where $K(\phi) = \frac{e^{-\frac{2\phi}{\alpha}} (\alpha^2+1)}{(\alpha^2+\beta+1)e^{-\frac{2\phi(\alpha^2+1)}{\alpha}} + \beta\alpha^2}$ can be expanded into series with respect to β

$$K(\phi) = e^{2\phi\alpha} - \frac{\left(e^{\frac{4\phi\alpha^2+2\phi}{\alpha}} \alpha^2 + e^{2\phi\alpha} \right) \beta}{\alpha^2 + 1} + \frac{\left(\frac{6\phi\alpha^2+4\phi}{\alpha} \alpha^4 + 2e^{\frac{4\phi\alpha^2+2\phi}{\alpha}} \alpha^2 + e^{2\phi\alpha} \right) \beta^2}{(\alpha^2 + 1)^2} + \dots \quad (12)$$

It is a combination of various dilaton field with different coupling strength. We'll later emphasize this point in the case of $\alpha = 1$ in Section IV. **A.** We can solve equations (4)-(6) to first order in the angular parameter ϵ . Following the method of [25], we also assume the unique term in the metric that changes to $O(\epsilon)$ is $g_{t\phi}$, the scalar field does not change to the order of $O(\epsilon)$, and A_ϕ is the only component of the vector potential that changes to the order of $O(\epsilon)$.

Therefore, we assume the metric being of the following form

$$ds^2 = -U dt^2 + \frac{1}{U} dr^2 - 2\epsilon k(r) \sin^2 \theta dt d\phi + f^2 d\Omega_2^2, \quad (13)$$

with

$$U = \left[1 - \left(\frac{b}{r} \right) \right] \left[1 - \left(\frac{a}{r} \right) \right]^{1-\gamma} + \beta q^2 \left\{ r^2 \left[1 - \left(\frac{a}{r} \right) \right]^\gamma \right\}^{-1}, \quad (14)$$

$$\gamma \equiv \frac{2\alpha^2}{\alpha^2+1}, q^2 = \frac{ab}{1+\alpha^2}.$$

The scalar and electric potential ϕ should be

$$\phi = -\frac{\alpha}{(\alpha^2 + 1)} \ln \left[1 - \left(\frac{a}{r} \right) \right], A_\mu = (A_t, 0, 0, -aqB(r) \sin(\theta)^2). \quad (15)$$

Inserting the metric, the Maxwell fields and the scalar field into field equations leads to the perturbation equations

$$\begin{aligned} & \frac{-k(r)}{f(r)^2} + \frac{k(r)f'(r)U'(r)}{f(r)} + \frac{U(r)k''(r)}{2} \\ & = \left(\frac{V(\phi)}{2} - \frac{K(\phi)}{2} (-2A_t'^2) \right) (-k(r)) + 2K(\phi) (-qU(r)A_t'(r)B'(r)) , \end{aligned} \quad (16)$$

and

$$\partial_r \left(- (k(r)A_t'(r) + qU(r)B'(r)) K(\phi) \right) + \frac{2qB(r)K(\phi)}{f(r)^2} = 0 . \quad (17)$$

Combing the equation of $R_{\theta\theta}$ and electromagnetic field

$$1 - Uf'^2 - U'ff' - Uff'' = \left[\frac{V}{2} - \frac{K}{2} (-2A_t'^2) \right] f^2 , \quad (18)$$

with

$$K(\phi) = \frac{-q}{f^2 A_t'} , \quad (19)$$

we find equations (16) and (17) can be reduced to

$$\frac{k''f^2}{2} = kf'^2 + kff'' + 2q^2B' , \quad (20)$$

and

$$\frac{d\left(\frac{k}{f^2}\right)}{dr} - \frac{d(UB'K(\phi))}{dr} + \frac{2BK(\phi)}{f^2} = 0 . \quad (21)$$

Integrate (20) and we achieve

$$f^2k' - (f^2)'k = 4q^2B + const . \quad (22)$$

Inserting it into equation (21), we obtain

$$\frac{4q^2B + const}{f^4} - \frac{d(UB'K(\phi))}{dr} + \frac{2BK(\phi)}{f^2} = 0 . \quad (23)$$

III. METHODOLOGY FOR SOLVING THE EQUATION

We'll later see that the angular momentum of the spacetime is proportional to the *const*. This means we must determine the value of *const*. As usual, we require the solutions have the behaviour of $k(r) \rightarrow c/r$ and $B(r) \rightarrow 1/r$ when $r \rightarrow \infty$.

Solving equation (22), we obtain

$$k = f^2 \int \frac{4q^2B + const}{f^4} + c_1 f^2 . \quad (24)$$

The asymptotical behaviour requires c_1 must vanish since $k(r) \rightarrow c/r$ at infinity.

Now we focus on the equation of B , i.e. equation (23). First, we search for the Frobenius series solution of $B(r)$ at infinity. Using the reciprocal substitution $r = 1/y$, we transform equation (23) into

$$\frac{4q^2B + const}{f^4} + y^2 \frac{\partial \left(-Uy^2 \frac{\partial B}{\partial y} K(\phi) \right)}{\partial y} + \frac{2BK(\phi)}{f^2} = 0 . \quad (25)$$

For the sake of calculation of the coefficients in the series, we multiply equation (25) by $f^4/K(\phi)^2$ and then the equation is transformed into

$$\frac{4q^2B + \text{const}}{K(\phi)^2} - \frac{y^4 f^4 U}{K(\phi)} \frac{d^2 B}{dy^2} - \frac{d(Uy^2 K(\phi))}{dy} \frac{f^4}{K(\phi)^2} y^2 \frac{dB}{dy} + \frac{2Bf^2}{K(\phi)} = 0. \quad (26)$$

By expanding the coefficients of $\frac{d^2 B}{dy^2}$, $\frac{dB}{dy}$ and B at $y = 0$, one finds they are in the order of $O(1)$, $O(1/y)$ and $O(1/y^2)$, respectively. This shows $y = 0$ is a regular singular point of the equation. Two roots of the indicial equation of the concerning homogeneous equation are -2 and 1 , respectively. So we shall exclude the exponent -2 since we need $B(y) = O(y)$ at $y = 0$. Therefore, we substitute

$$B(y) = y \sum_{n=0}^{\infty} c_n y^n, \quad (27)$$

into equation (26) and the coefficient of y^0 gives

$$\beta^2 \text{const} + (((-\gamma + 3)a + 3b) c_0 - 4 c_1 + 2 \text{const}) \beta + ((-2\gamma + 3)a + 3b) c_0 - 4 c_1 + \text{const} = 0. \quad (28)$$

As usual, we require $c_0 = 1$ and there are still two variables, const and c_1 to be determined. The equations of higher order will introduce c_2, c_3 and so on. And thus it indicates the equations of coefficients are not closed.

When $\beta = 0$, Sheykhi gives a particular solution, $B(r) = 1/r$ in [28]. In [42], Barausse et al make a study on a slowly rotating black holes in Einstein-aether theory where they impose the condition that the solutions are regular everywhere, except for their center (singularity of the black hole). Equation (26) exhibits apparent singularities on the horizon of the black holes with $U = 0$. If the solution is to be regular there, $B'(r)$ and $B(r)$ should satisfy the following equation on the horizon,

$$\left[\frac{4q^2B + \text{const}}{K(\phi)^2} - \frac{d(Uy^2 K(\phi))}{dy} \frac{f^4}{K(\phi)^2} y^2 \frac{dB}{dy} + \frac{2Bf^2}{K(\phi)} \right]_{y=y_h} = 0. \quad (29)$$

Combining this condition and the asymptotic behavior of $B(r)$ at infinity, we are able to specify the exact value of const . However, it should be noticed that there is not one but two horizons in the general case. Actually, there will be two horizons ($r_h > a$) as long as $0 < \beta q^2 < \frac{(b-a)^2}{4}$. In general, when more than one horizon exist, one expects them to be singular in the equation. As we have discussed above, in order to preserve the regularity on the horizon, we need to impose the local regularity condition. So, if there are two horizons, one has to impose two local conditions. However, with one regular condition alone, the solution is already specified without any other parameters to tune for imposing further regularity conditions. Although solutions with multiple horizons will exhibit multiple singularities on the horizons, it is enough to impose the regular condition only on the outermost horizon. This is acceptable from a phenomenological view of point, the outermost horizon can be rendered regular by using the usual regularity condition while the remaining singularities are hidden in the outermost horizon.

Indeed, in the case of $\beta = 0$, $B(r) = \frac{1}{r}$ is the unique solution that satisfy the corresponding regular condition.

In order to solve the equations numerically, we first set $\text{const} = 1$ by rescaling $B(r)$, imposing the boundary condition (29) and $B(0) = 0$ where $y_h = \left(a/2 + b/2 + 1/2 \sqrt{2ab\beta\gamma - 4ab\beta + a^2 - 2ab + b^2} \right)^{-1}$. We extract $B'(0)$ from the numerical solution once we complete it. Then we obtain the exact value of $\text{const} = 1/B'(0)$ since we require $B(y) \sim y$ at $y = 0$. When $\beta = 0$, we find $\text{const} = (2\gamma - 3)a - 3b$ and we see the const depends linearly on γ .

IV. THE CASE OF NORMAL COUPLING WITH $\beta \geq 0$

In this section we investigate the case of $\beta \geq 0$ where the sign of $K(\phi)$ is always positive in the whole spacetime. Otherwise, there would exist regions where $K(\phi) < 0$ which corresponds to phantom Maxwell field which we will consider in the later section as an exact slowly rotating solution.

A. angular momentum, gyromagnetic ratio and angular velocity

Now let's concentrate on the effects of β on const . We fix $a = 1, b = 3$ and $\beta = 0, 0.2, 0.4, 0.6, 0.8$, respectively. Then we make the research on the relation between const and γ and the relation is plotted in Fig. 1.

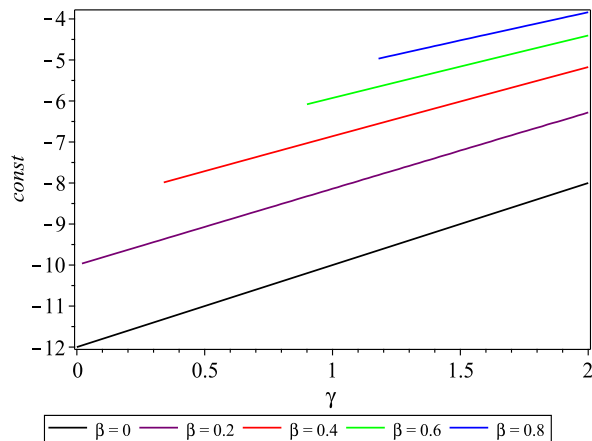


FIG. 1: The relation between $const$ and γ . The parameters are $a = 1$, $b = 3$.

The figure shows that several curves cannot be extended into $\gamma = 0$ since we should require $0 < \beta q^2 < \frac{(b-a)^2}{4}$. Otherwise, there will be naked singularity which violates the cosmic censorship conjecture. Considering $\gamma = \frac{2\alpha^2}{\alpha^2+1}$, one will find the range of γ is $[0, 2)$. Once we get the numerical value of $const$, we can achieve a truncated series solution of $B(y)$.

As a final check, our numerical solution is compared with series solution to $B(y)$ in Fig. 2.

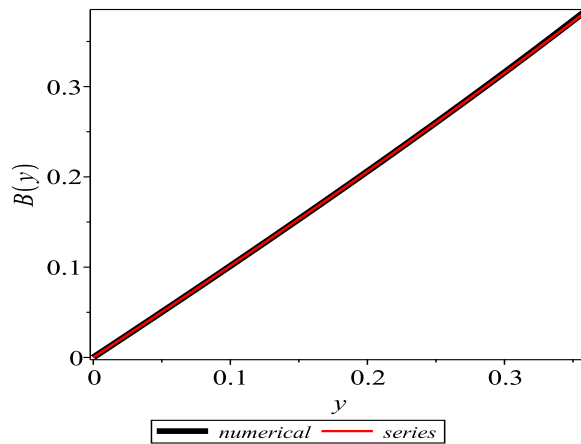


FIG. 2: The numerical and the series solution for the relation B and y . The parameters are $a = 1$, $b = 3$, $\gamma = 1$, $\beta = 1/4$. The truncated series solution is $y + 0.12056y^2 + 0.12404y^3 + 0.12748y^4$.

In the next, we calculate the angular momentum of the slowly rotating black hole. It can be calculated using the method provided by Brown and York [43]. Conserved charges such as angular momentum are defined using the surface stress tensor and Killing vector fields on the boundary of spacetime. To be exact, the spacetime region M is topologically the product of a three-space Σ and a real interval. The boundary of Σ is B and the product of B with segments of timelike world lines orthogonal to Σ at B is denoted as 3B .

The surface stress energy tensor is defined by

$$\tau^{ab} = \frac{1}{8\pi} (\Theta^{ab} - \Theta\gamma^{ab}), \quad (30)$$

which is derived from the variation of the action with respect to the 3B metric γ^{ab} .

The boundary 3B is foliated by a family of spacelike two-surfaces. Then we can decompose the boundary metric γ^{ab} into standard ADM form:

$$\gamma_{ab}dx^a dx^b = -N^2 dt^2 + \sigma_{ij} (d\varphi^i + V^i dt) (d\varphi^j + V^j dt), \quad (31)$$

where we have chosen the two-surface as a two-sphere, and the coordinates φ^i are the angular variables parameterizing the hypersurface of constant r around the origin. N and V^i are the lapse and shift functions, respectively.

Suppose the boundary of three-metric γ^{ab} possesses an isometry concerned with Killing vector field ξ on the boundary, then the corresponding conserved charge is defined by

$$Q(\xi) = \int_{\mathcal{B}} d^2\varphi \sqrt{\sigma} \tau_{ab} n^a \xi^b, \quad (32)$$

where n^a is the normal vector of B and tangent to 3B .

For boundary with rotational Killing vector field, the conserved charge is angular momentum,

$$J = \int_{\mathcal{B}} d^2\varphi \sqrt{\sigma} \tau_{ab} n^a \left(\frac{\partial}{\partial \varphi} \right)^b. \quad (33)$$

Expanding $\tau_{ab} n^a \left(\frac{\partial}{\partial \varphi} \right)^b$ and collecting the terms of order $O(\epsilon)$, we obtain

$$\tau_{ab} n^a \left(\frac{\partial}{\partial \varphi} \right)^b = \sin^2\theta \frac{(-2kf'(r) + f(r)k'(r)) \epsilon}{16\pi f(r)}. \quad (34)$$

Perform the integration and now the angular momentum equals to

$$J = \lim_{r \rightarrow \infty} -\frac{1}{6} (q^2 B + \text{const}) \epsilon. \quad (35)$$

Taken account of $B(r) = O(1/r)$ at infinity, the angular momentum equals to $-\epsilon \frac{\text{const}}{6}$. Angular momentum can also be calculated by means of the Komar angular momentum. Then the same value is achieved (for details see [44]). When $\beta = 0$, we have $\text{const} = (2\gamma - 3)a - 3b$ and the angular momentum is

$$J = \frac{\epsilon}{2} \left(b + \frac{3 - \alpha^2}{3(1 + \alpha^2)} a \right), \quad (36)$$

which is the same as the value in [28].

Once we get the numerical value of const , we can calculate the gyromagnetic ratio of the black hole. One of the remarkable facts about a Kerr-Newman black hole is that it has a gyromagnetic ratio $g = 2$, just as an electron in the Dirac theory. Scalar field such as the dilaton, modify the value of gyromagnetic ratio of the black hole. As a result, it doesn't possess the gyromagnetic ratio of $g = 2$ [25]. Now we focus on the influence of β on the gyromagnetic ratio g .

The charge of the black hole Q coincides with q in four dimensions, see [40].

$$Q = q = \sqrt{\frac{ab}{1 + \alpha^2}} = \frac{\sqrt{2}\sqrt{-ba(\gamma - 2)}}{2}. \quad (37)$$

The magnetic dipole moment for this asymptotically AdS slowly rotating black hole can be defined as

$$\mu = Q\epsilon = g \frac{QJ}{2M}. \quad (38)$$

Substituting $M = \frac{1}{2} (b + (1 - \gamma)a)$ in [40] and $J = -\frac{\epsilon}{6} \text{const}$ into above equation, we obtain $g = -6 \frac{(b + (1 - \gamma)a)}{\text{const}}$.

We have shown the behavior of the gyromagnetic ratio g of the black holes versus γ in Fig. 3. From this figure we find that the gyromagnetic ratio decreases with γ or α with fixed value of β . However, when γ is fixed, the gyromagnetic ratio increases with β . Taking $\gamma = 0$ as an example, one finds when $\beta \leq \frac{(a-b)^2}{4ab}$ and the black hole has an event horizon which hides the singularity so that the singularity is not naked. In this case we have $B(r) = 1/r$ and $\text{const} = -\frac{(3a+3b)}{\beta+1}$. Therefore, the gyromagnetic ratio is $2(\beta + 1)$. We thus conclude undoubtedly that the non-vanishing positive β increases the gyromagnetic ratio. Furthermore, the gyromagnetic ratio of the Kerr-Newman black hole can be also realized in the Einstein-Maxwell-scalar black hole by increasing the value of β and γ at the same time.

In the next, for simplicity, we will restrict ourselves to the case of $\gamma = 1$, i.e., $\alpha = 1$. Then the corresponding action is [39, 41]

$$S = \int dx \sqrt{-g} \left(R - 2\nabla_\mu \phi \nabla^\mu \phi - \frac{2e^{2\phi}}{\beta + 2 + \beta e^{4\phi}} F^2 \right). \quad (39)$$

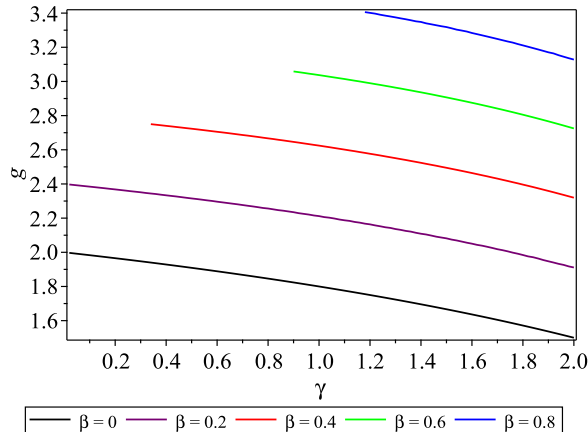


FIG. 3: The gyromagnetic ratio with respect to γ . The parameters are $a = 1$, $b = 3$,

The resulting line element of the black hole spacetime is

$$ds^2 = - \left(1 - \frac{2M}{r} + \frac{\beta Q^2}{f^2} \right) dt^2 + \frac{dr^2}{\left(1 - \frac{2M}{r} + \frac{\beta Q^2}{f^2} \right)} + f^2 d\Omega^2, \quad (40)$$

with

$$f = r \left(1 - \frac{Q^2}{Mr} \right)^{\frac{1}{2}}. \quad (41)$$

Expand $K(\phi)$ in terms of β

$$K(\phi) = \frac{2e^{2\phi}}{\beta + 2 + \beta e^{4\phi}} = e^{2\phi} - \frac{(e^{4\phi} + 1) e^{2\phi} \beta}{2} + \frac{e^{2\phi} (e^{4\phi} + 1)^2 \beta^2}{4} + \dots, \quad (42)$$

one finds that $K(\phi)$ is actually the combination of infinite and different dilaton couplings.

We have presented the gyromagnetic ratio of the slowly rotating black hole with respect to $\frac{Q}{M}$ for different value of β in Fig. 4. The black line corresponds to the standard dilaton field $K(\phi) = e^{2\phi}$, and the other lines correspond to the superposition of various dilaton fields. It shows that the gyromagnetic ratio increases with β but decreases with $\frac{Q}{M}$. This means we can achieve the same ratio of Kerr-Newman black holes by increasing β and charge-to-mass ratio at the same time.

In the next, it is our turn to study the angular velocity of black hole horizon. The coordinate angular velocity of a locally nonrotating observer, with four velocity u^μ such that $u_{\xi\phi} = 0$ is given by $\Omega = -\frac{g_{t\phi}}{g_{\phi\phi}} = \epsilon \frac{k(r)}{f(r)^2}$. It is known that one of the important quantities is the angular velocity of the horizon Ω_h , which affects the region where the super-radiance occurs in the black hole background.

For the slowly rotating charged Kerr black hole, the angular velocity of the horizon is equal to $\epsilon \frac{1}{r_h^2}$. For this reason we can nondimensionalize the angular velocity. In Fig. 5, we show the dependence of dimensionless angular velocity of the horizon with respect to the charge-to-mass ratio.

We find the upper limit for $\frac{Q}{M}$ for fixed β is

$$\sqrt{(2\beta + 2) - 2\sqrt{\beta(\beta + 2)}}, \quad (43)$$

in order to ensure the singularity $r = \frac{Q^2}{M}$ of the black hole is not naked. One can see that for fixed β , the dimensionless angular velocity of the horizon increases with the charge-to-mass ratio. Nevertheless, when $\frac{Q}{M}$ is fixed, the angular velocity decreases with β . Therefore, one can achieve the angular velocity of the event horizon which is the same as that in charged Kerr black holes by increasing the value of β and $\frac{Q}{M}$ simultaneously.

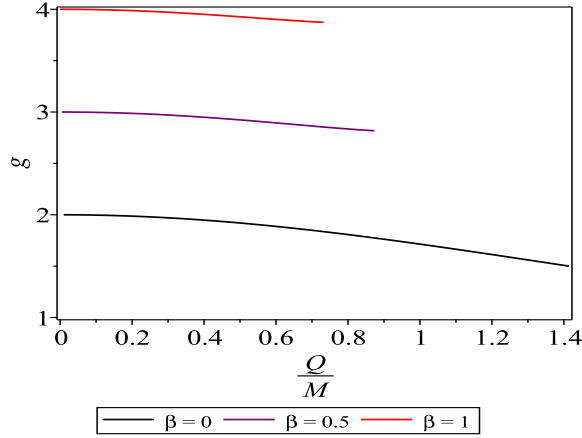


FIG. 4: The gyromagnetic ratio with respect to $\frac{Q}{M}$ for different value of β .

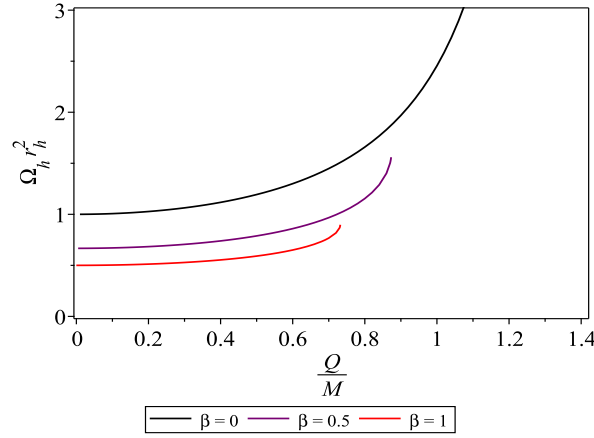


FIG. 5: The dimensionless angular velocity of the horizon with respect to charge-to-mass ratio for different values of β . ϵ is set to 1.

B. The innermost stable circular orbit, the radiation efficiency and their corrections

In this section, we will focus on the circular orbits in the equatorial plane in order to investigate the geometry of the spacetime above. In the stationary and axially symmetric spacetime, one can find the geodesics take the form [45].

$$\begin{aligned}
 \dot{t} &= \frac{-Eg_{\phi\phi} - L_z g_{t\phi}}{-g_{t\phi}^2 + g_{tt}g_{\phi\phi}}, \\
 \dot{\phi} &= \frac{-Eg_{t\phi} - L_z g_{tt}}{g_{t\phi}^2 - g_{tt}g_{\phi\phi}}, \\
 g_{rr}\dot{r}^2 + g_{\theta\theta}\dot{\theta}^2 &= V_{eff}(r, \theta; E, L_z),
 \end{aligned} \tag{44}$$

with the effective potential

$$V_{eff}(r) = \frac{E^2 g_{\phi\phi} + 2EL_z g_{t\phi} + L_z^2 g_{tt}}{g_{t\phi}^2 - g_{tt}g_{\phi\phi}} - 1, \tag{45}$$

where the overhead dot stands for the derivative with respect to the affine parameter, and the constants E and L_z correspond to the conserved energy and the (z-component of) orbital angular momentum of the particle, respectively.

For simplicity, we put the orbits on the equatorial plane. With the restriction that $\theta = \frac{\pi}{2}$, one can find for the

stable circular orbit in the equatorial plane, the effective potential $V_{eff}(r)$ must obey

$$V_{eff}(r) = 0, \quad \frac{dV_{eff}(r)}{dr} = 0. \quad (46)$$

Solving above equations, one obtain

$$\begin{aligned} E &= \frac{-g_{tt} - g_{t\phi}\Omega}{\sqrt{-g_{tt} - 2g_{t\phi}\Omega - g_{\phi\phi}\Omega^2}}, \\ L_z &= \frac{g_{t\phi} + g_{\phi\phi}\Omega}{\sqrt{-g_{tt} - 2g_{t\phi}\Omega - g_{\phi\phi}\Omega^2}}, \\ \Omega &= \frac{d\phi}{dt} = \frac{-g_{t\phi,r} + \sqrt{(g_{t\phi,r})^2 - g_{tt,r}g_{\phi\phi,r}}}{g_{\phi\phi,r}}. \end{aligned} \quad (47)$$

Then the corrections to energy, angular momentum and period up to first order of ϵ are

$$E^2 = \frac{U^2 (f^2)'}{U (f^2)' - f^2 U'} + \epsilon \cdot \frac{2U \sqrt{U' (f^2)' f^2 (k'U - kU')}}{(-U' f^2 + U (f^2)')^2}, \quad (48)$$

$$L^2 = \frac{f^4 U'}{U (f^2)' - U' f^2} + \epsilon \cdot \frac{-2f^2 U \sqrt{U' (f^2)' (-k' f^2 + (f^2)' k)}}{(-U' f^2 + U (f^2)')^2}, \quad (49)$$

$$T^2 = T_0^2 + \epsilon T_1^2 = \frac{4\pi^2 (f^2)'}{U'} - 4\pi^2 \epsilon \cdot \frac{2 (f^2)' k'}{\sqrt{U' (f^2)' U'}}. \quad (50)$$

We don't bother to show the detailed formula for energy, angular momentum and orbital period since they are too lengthy. The relative correction of the period

$$\Delta T^2 = \frac{T_1^2}{T_0^2} = -\frac{2k'}{\sqrt{U' (f^2)'}}, \quad (51)$$

is shown in Fig. 6. One can see that for fixed values of radius for circular orbits and fixed β , the relative correction of

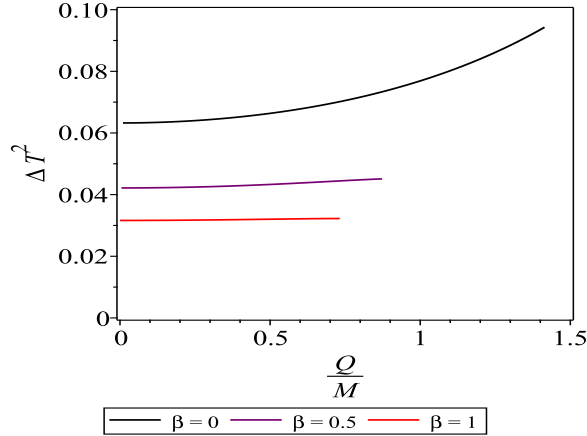


FIG. 6: The corrected period with respect to $\frac{Q}{M}$ for different values of β . The radius of circular orbit is set to $10M$ and $\epsilon = 1$.

the period increases with $\frac{Q}{M}$. The correction becomes smaller and smaller with the increasing of β .

The innermost stable circular orbit (ISCO) of the particle around the black hole is given by the equation $V_{eff,rr} = 0$, i.e.

$$E^2 g''_{\phi\phi} + 2EL_z g''_{t\phi} + L_z^2 g''_{tt} = (g_{t\phi}^2)'' - (g_{tt} g_{\phi\phi})'' . \quad (52)$$

Substituting the expressions for E and L_z from (47) and the expressions for $g_{tt}, g_{t\phi}, g_{\phi\phi}$, into Eq. (52), we obtain the equation which is denoted by $F(r, \epsilon) = 0$. As usual, we assume R is the radius of ISCO in static spacetime, i.e., $F(R, 0) = 0$. Then the correction of radius of ISCO up to first order of ϵ for the slowly rotating black hole is $R + \epsilon R_1$. Here $R_1 = -\frac{F_2(R, 0)}{F_1(R, 0)}$ and $F_1(R, 0)$ and $F_2(R, 0)$ represent the derivative with respect to the first and second variable, respectively.

Again, we don't bother to give the expression for R since it is the root of a quartic equation. But we plot the radius of innermost stable circular orbits with respect to $\frac{Q}{M}$ for different values of β in Fig. 7(a). The relative correction, i.e. $\frac{R_1}{R}$ is also shown in Fig. 7(b). The figure shows that the relative corrections of radius of innermost stable circular

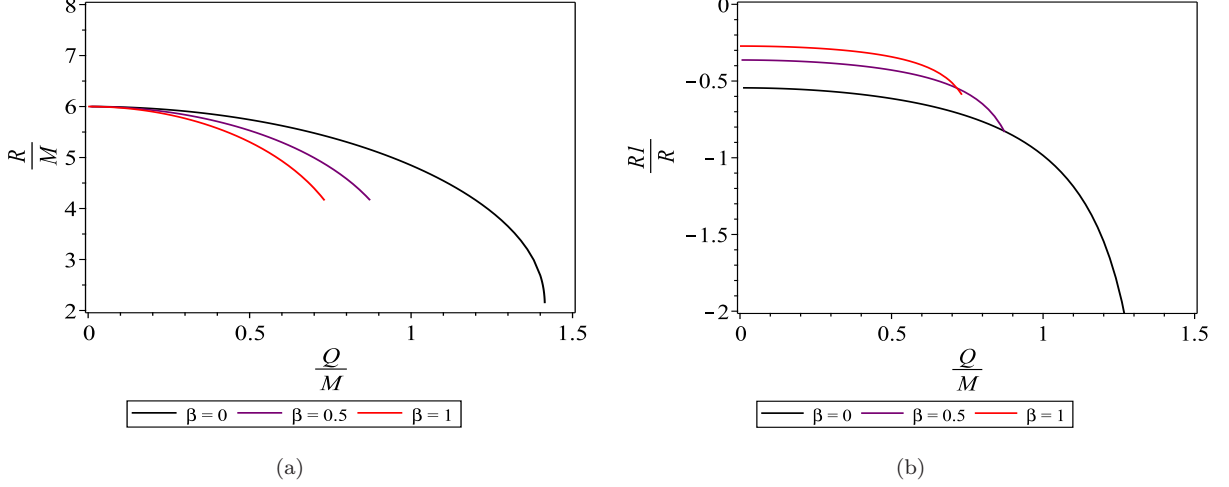


FIG. 7: (a) The dimensionless radius of innermost stable circular orbits with respect to $\frac{Q}{M}$ for different values of β . (b) The relative correction to dimensionless radius of innermost stable circular orbits with respect to $\frac{Q}{M}$ for different values of $\beta = 0, 0.5, 1$, respectively.

orbits are always negative when the perturbation parameter $\epsilon > 0$, and the absolute value increases with respect to the charge-to-mass ratio. The relative corrections become smaller and smaller with the increasing of β .

Let us turn now to the computation of the effect for β on the radiative efficiency η , in the thin accretion disk model, which is defined by

$$\eta = 1 - E(R_{ISCO}). \quad (53)$$

This quantity represents the maximum fraction of energy being radiated when the test particle is accreted by a central black hole. For the Schwarzschild black holes and the extreme Kerr black holes, the radiative efficiencies are 0.057 and 0.42, respectively. It's easy to prove that $E_1(R, 0)$ vanish for radius of ISCO, since the expression for $E_1(R, 0)$ equals equation of RISCO multiplied by something.

From equation(47), we know the energy is

$$E(R_{ISCO}) = E(R + \epsilon R_1, \epsilon) \approx E(R) + \epsilon(E_1(R, 0) + E_2(R, 0)). \quad (54)$$

Now we denote $1 - E(R)$ and $-\epsilon(E_1(R, 0) + E_2(R, 0))$ by η_0 and η_1 , respectively.

The figure shows that the radiative efficiency η_0 of the rotating black hole increases starting from $1 - \frac{2\sqrt{2}}{3} \approx 0.057$ with the increasing of $\frac{Q}{M}$ for fixed value of β . On the other hand, for the fixed $\frac{Q}{M}$, the radiative efficiency η_0 increases with the increasing of β . As for the first order correction to radiative efficiency, η_1 , the figure shows that the correction increases with respect to $\frac{Q}{M}$ for fixed β . And for fixed $\frac{Q}{M}$, the radiative efficiency increases with the increasing of $\frac{Q}{M}$.

Taking the zeroth order efficiency, η_0 and the first order efficiency, η_1 into account, we obtain the total efficiency up to first order in Fig. 9. From Fig. 9, we can see that for small values of β and $\epsilon < 0$, the efficiency will vanish for some value of $\frac{Q}{M}$. In this situation, the black hole's capability of capturing particles becomes so weak that the accreted matter around it is greatly diluted. This leads to radiation can not be generated because of the lacking of enough stress and dynamic friction in the accretion disk model.

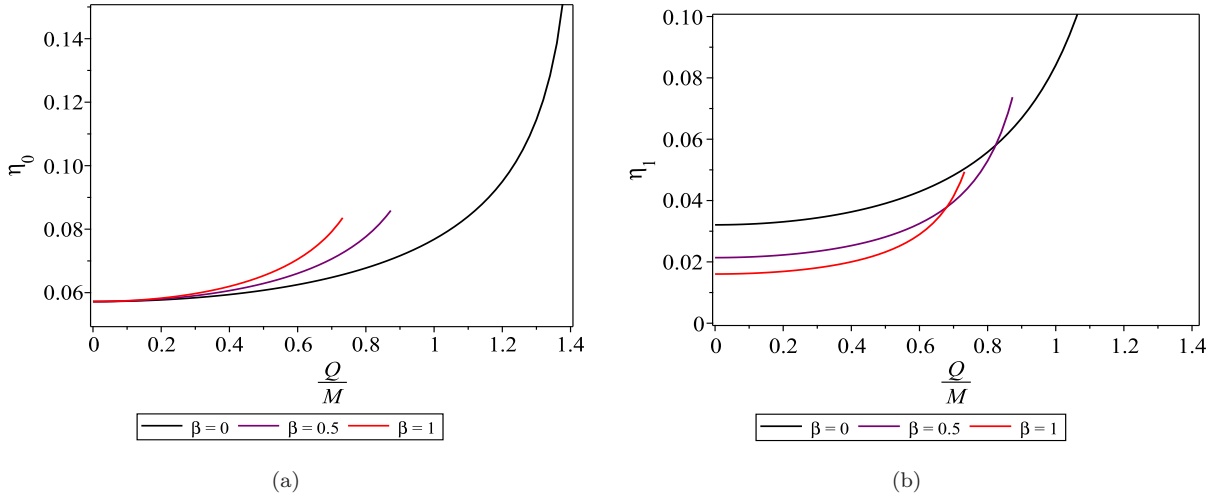


FIG. 8: (a) The radiation efficiency η_0 with respect to $\frac{Q}{M}$ for different values of β in the static spacetime. (b) The first order corrections η_1 to radiation efficiency with respect to $\frac{Q}{M}$ for different values of β .

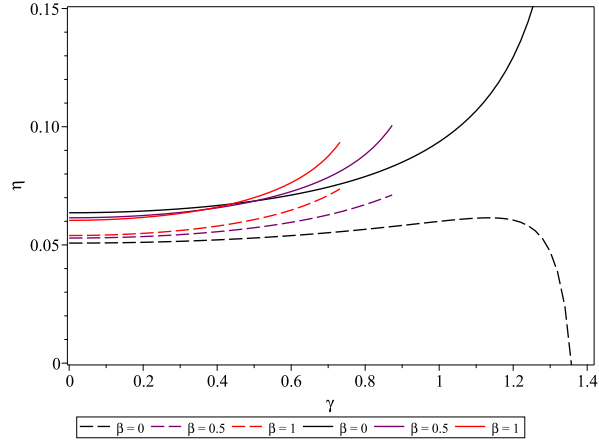


FIG. 9: The evolution of total efficiency η up to first order with respect to $\frac{Q}{M}$ for different value of β . The solid and dashed lines corresponds to $\epsilon = 0.2$ and $\epsilon = -0.2$, respectively.

V. THE CASE OF PHANTOM COUPLING WITH $\beta < 0$: AN EXACT SLOWLY ROTATING PHANTOM SOLUTION

When $\beta = \frac{2}{\gamma-2}$, the action of the theory reduces to

$$S = \int d^4x \sqrt{g} \left(R - 2\nabla_u \phi \nabla^u \phi + \frac{e^{-\frac{2\phi}{\alpha}}}{\alpha^2} F^2 \right), \quad (55)$$

which implies that we are investigating a phantom Maxwell field because the sign before the Maxwell invariant becomes positive. One can also make transformations $\phi \rightarrow I\phi$ and $\alpha \rightarrow I\alpha$ such that the sign before Maxwell invariant is not changed while the scalar field is presented as a phantom scalar field.

$$S = \int d^4x \sqrt{g} \left(R + 2\nabla_u \phi \nabla^u \phi - \frac{e^{-\frac{2\phi}{\alpha}}}{\alpha^2} F^2 \right) \quad (56)$$

Further more, if we make transformations, $\frac{\phi}{\alpha} \rightarrow \phi, \frac{F^2}{\alpha^2} \rightarrow F^2$ The action becomes

$$S = \int d^4x \sqrt{g} (R + 2\alpha^2 \nabla_u \phi \nabla^u \phi - e^{-2\phi} F^2) , \quad (57)$$

which differs from the Einstein-Maxwell-dilaton theory by the kinetic term. Now return to action (55) we have the black hole solution as follows

$$U(r) = \frac{r - (a + b)}{r(1 - \frac{a}{r})^\gamma} . \quad (58)$$

Therefore the radius of the event horizon locates at $r_+ = a + b$. Solving for $B(r)$ in Eq. (23) with the asymptotic boundary conditions and the regular conditions, we obtain $B(r) = \frac{1}{r-a}$ and

$$const = \frac{(\gamma - 2)(2a\gamma - a - 3b)}{\gamma} . \quad (59)$$

Then the corresponding gyromagnetic ratio is exactly

$$g = 6 \frac{\gamma ((\gamma - 1)a - b)}{(\gamma - 2)(2a\gamma - a - 3b)} . \quad (60)$$

Observing the metric, we find we can always set $a = 1$ by rescaling r . In the next, we will research on various properties when the charge-to-mass ratio is fixed. But before that, let's first research on charge-to mass ratio which takes the form

$$\frac{Q}{M} = -\frac{\sqrt{2}\sqrt{-ab(\gamma-2)}}{a(\gamma-1)-b} = -\frac{\sqrt{2}\sqrt{-b(\gamma-2)}}{\gamma-1-b} . \quad (61)$$

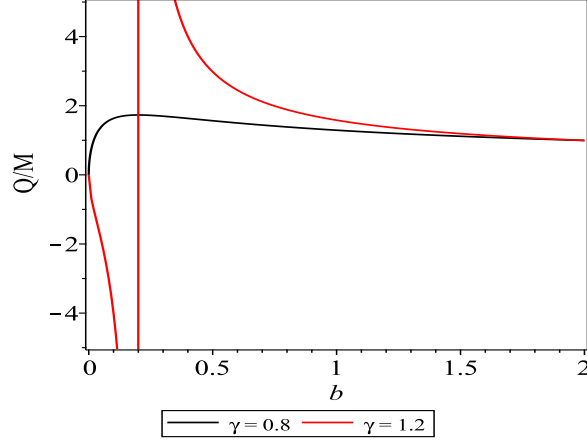


FIG. 10: The charge-to-mass ratio with respect to γ . The black and red lines correspond to $\gamma = 0.8$ and $\gamma = 1.2$, respectively

Two representative curves of charge-to-mass ratio are shown in Fig. 10. When $\gamma < 1$, the denominator of the expression for Q/M will never vanish, and the value of Q/M is bounded. Concretely, when $b = 1 - \gamma$, Q/M achieves the maximum of $\sqrt{\frac{\gamma-2}{2\gamma-2}}$. This reveals that when $Q/M < \sqrt{\frac{\gamma-2}{2\gamma-2}}$, there will be two values of b correspond to the same charge-to-mass ratio which we denote them by small black hole and large black hole, respectively. Let's denote Q/M by κ , then the expression for small b is

$$b_1 = \frac{-\sqrt{-4((\kappa^2 - 1/2)\gamma - \kappa^2 + 1)(\gamma - 2)}\sqrt{2} + (2\gamma - 2)\kappa^2 - 2\gamma + 4}{2\kappa^2} , \quad (62)$$

and the large b is

$$b_2 = \frac{\sqrt{-4((\kappa^2 - 1/2)\gamma - \kappa^2 + 1)(\gamma - 2)}\sqrt{2} + (2\gamma - 2)\kappa^2 - 2\gamma + 4}{2\kappa^2} . \quad (63)$$

For the case of $\gamma > 1$, the denominator will vanish when $b = \gamma - 1$. Therefore, the charge-to-mass ratio will diverge at this point as shown in Fig. 10. The left branch corresponds to negative charge-to-mass ratio while the right branch corresponds to the positive one. For a given $\kappa > 0$, there's only b_2 corresponding to this charge-to-mass ratio. On the other hand, for a given $\kappa < 0$, there's also only a b_1 corresponding to this charge-to-mass ratio. In this case, b_1 corresponds to charge-to-mass ratio of $-|\kappa|$. From now on, for simplicity, we shall focus on the absolute value of charge to mass ratio. So there will be two different b corresponding to the same value of charge-to-mass ratio no matter $\gamma < 1$ or not.

In all, when $\gamma > 1$, b_1 or small black hole represents the case of negative mass and b_2 or large black hole represents the case of positive mass.

Now, let's observe the evolution of gyromagnetic ratio with respect to γ when κ is fixed as shown in Fig. 11. We see that the large black holes and the small black holes with the same κ have the same range of γ , and the range shrinks with the increasing of charge-to-mass ratio. For any fixed value of κ , there's always a divergent point of g where the *const* vanishes, and the value of γ corresponding to the divergent point increases with the increasing of κ . When $\kappa < 1$, γ can take any value in $(0, 2)$. The gyromagnetic ratio first monotonically decreases to $-\infty$ and then jumps to $+\infty$ and decreases monotonically again. As for large black holes, the gyromagnetic ratio decreases monotonically to $-\infty$. When $\kappa > 1$, the range of γ shortens. For example, when $\kappa = 1.2$, the general trend of gyromagnetic ratio doesn't change. However, when $\kappa = 1.8$, the gyromagnetic ratio of small black holes decreases monotonically while for large black holes, it increases to the maximum and then decreases. When $\kappa = 4$, there's a divergent point for the gyromagnetic ratio for large black holes. The left branch increases monotonically and the right branch first increases and then decreases. For small black holes, the ratio monotonically decreases to $-\infty$.

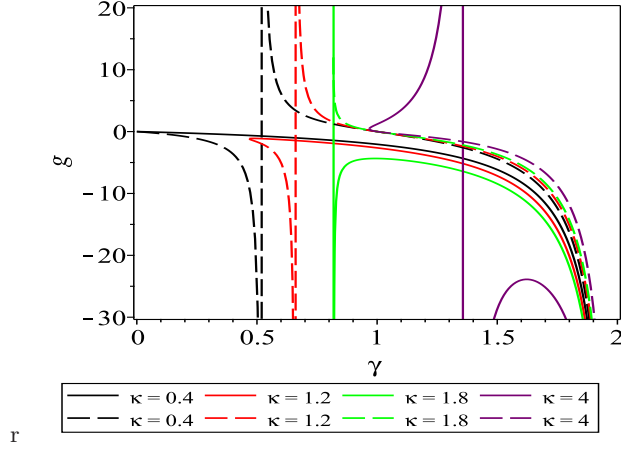


FIG. 11: The gyromagnetic ratio with respect to γ . The solid lines correspond to large black holes while the dashed lines correspond to small black holes, respectively.

With the expression for $B(r)$ from (24), we obtain

$$k(r) = \left\{ \left[a^2(a+b-r)\gamma^2 + \left(r^2a + \frac{a^2r}{2} - \frac{3(a+\frac{5}{3}b)a^2}{2} \right) \gamma - \frac{r^3}{2} + \frac{a^2(a+3b)}{2} \right] \cdot \left(1 - \frac{a}{r} \right)^{-\gamma} + \frac{\left(1 - \frac{a}{r} \right)^\gamma r^3}{2} \right\} \cdot \frac{2(\gamma-2)}{\gamma(2\gamma^2-5\gamma+3)ra^2}. \quad (64)$$

It seems that when $\gamma = 1, \frac{3}{2}$, the expression is undefined. But we shall show that it is not case. Actually, using the L'Hospital's rule, we find equation (64) reduces to

$$k(r) = \frac{2r(r-a)^2 \ln\left(1 - \frac{a}{r}\right) + (a^2 - (b+3r)a + 2r^2)a}{(r-a)a^2}, \quad (65)$$

when $\gamma = 1$, and

$$k(r) = -2r \left[(r-a)^3 \ln\left(1 - \frac{a}{r}\right) + \frac{3\left(a^2 + (b - \frac{5}{3}r)a + \frac{2^2}{3}\right)a}{2} \right] \cdot \frac{\sqrt{1 - \frac{a}{r}}}{3a^2(r-a)^2}, \quad (66)$$

when $\gamma = \frac{3}{2}$. Therefore, $\gamma = 1$ and $\gamma = \frac{3}{2}$ are not singularities and $k(r)$ is continuous in terms of γ . We don't investigate the case of $\gamma = 0$ (or $\beta = -1$) since in this case, the denominator of $K(\phi)$ vanishes and the action is not defined. We find it is interesting to investigate the case of small charge-to-mass ratio, i.e. $\kappa < 1$. Then γ can take any values in $(0, 2)$. In order to understand the behavior of $k(r)$ for large and small black holes, we make the reciprocal substitution $r = 1/y$ and then make graph of function $k(y)$ in Fig. 12.

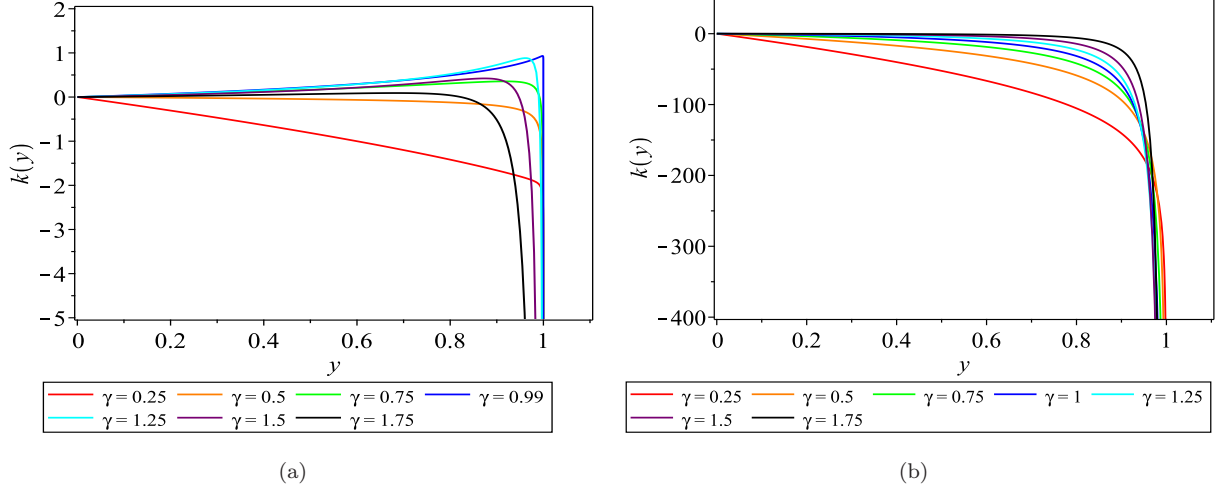


FIG. 12: (a) $k(y)$ with respect to y for the small black holes. (b) $k(y)$ with respect to y for the large black holes. The charge-to-mass ratios is set equal to 0.5.

From the figure, we see black holes of small size and large size exhibit different properties. For small black hole, with the increasing of γ from zero to 2, $k(y)$ decreases monotonically at first and then increases to a maximum and lastly decreases again. We note that the sign of $k(y)$ changes from negative to positive, which means the existence of vanishing angular velocity for local non-rotating observer.

For large black holes, the figure shows $k(y)$ is always negative and decreases monotonically with the increasing of y .

With the knowledge of $k(r)$, we can turn now to the coordinate angular velocity of a locally nonrotating observer which is given by

$$\Omega(r) = \left\{ \left[a^2(a+b-r)\gamma^2 + \left(r^2a + \frac{a^2r}{2} - \frac{3(a+\frac{5}{3}b)a^2}{2} \right) \gamma - \frac{r^3}{2} + \frac{a^2(a+3b)}{2} \right] \cdot \left(1 - \frac{a}{r} \right)^{-\gamma} + \frac{\left(1 - \frac{a}{r} \right)^\gamma r^3}{2} \right\} \cdot \frac{2(\gamma-2)}{\gamma(2\gamma^2-5\gamma+3)ra^2} \cdot \frac{1}{r^2 \left(1 - \frac{a}{r} \right)^\gamma}, \quad (67)$$

for general γ and

$$\Omega(r) = \frac{2r(r-a)^2 \ln \left(1 - \frac{a}{r} \right) + (a^2 - (b+3r)a + 2r^2) a}{(r-a)a^2} \frac{1}{r^2 \left(1 - \frac{a}{r} \right)}, \quad (68)$$

for $\gamma = 1$, and

$$\Omega(r) = -2r \left[(r-a)^3 \ln \left(1 - \frac{a}{r} \right) + \frac{3(a^2 + (b-\frac{5}{3}r)a + \frac{2r^2}{3})a}{2} \right] \cdot \frac{\sqrt{1-\frac{a}{r}}}{3a^2(r-a)^2} \cdot \frac{1}{r^2 \left(1 - \frac{a}{r} \right)^{\frac{3}{2}}}, \quad (69)$$

for $\gamma = \frac{3}{2}$. For convenience, we shall consider the dimensionless angular velocity of the event horizon $\tilde{\Omega}_h = \frac{\Omega_h}{(a+b)^2}$ with respect to γ but $\frac{Q}{M}$ is specified.

In Fig. 13, we plot the evolution of dimensionless angular velocity with respect to γ . We can see that the dimensionless angular velocity of event horizon are negative for both small black holes and large black holes. For small black hole, the angular velocity on the event horizon exhibits different properties in the case of $\gamma < 1$ and $\gamma > 1$. $\gamma = 1$ is a divergent point since there doesn't exist small black hole. We see that for small black hole, when $\gamma > 1$ and the

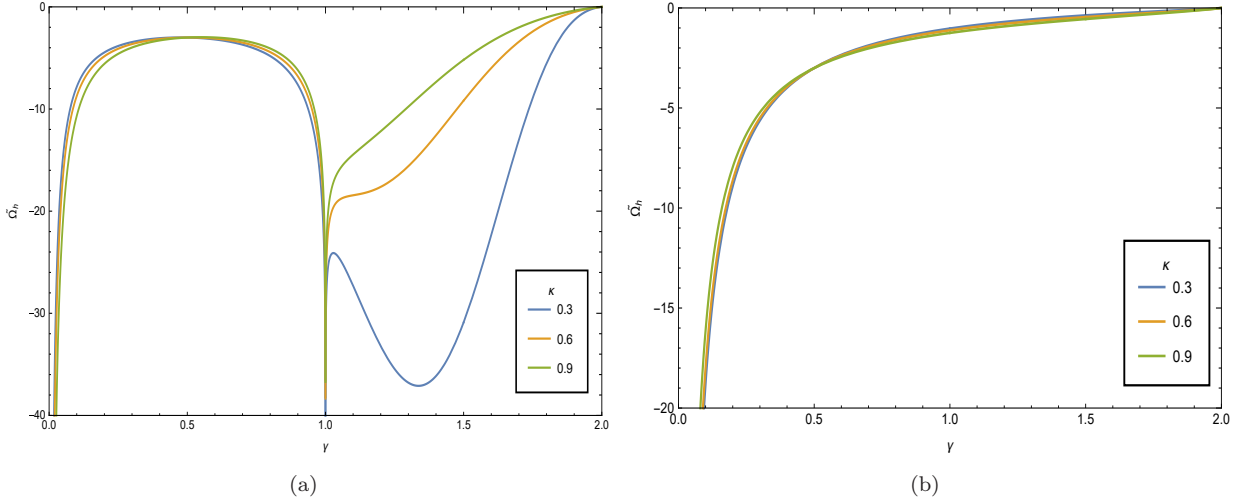


FIG. 13: (a) The dimensionless angular velocity on the event horizon with respect to γ for the small black holes. (b) The dimensionless angular velocity on the event horizon with respect to γ for the large black hole. The charge-to-mass ratios is set equal to 0.3, 0.6, 0.9, respectively.

charge-to-mass ratio is small, for example, $\kappa = 0.3, 0.6$, the absolute value of angular velocity decreases from $\gamma = 1$ at first and then increases to a local maximum and lastly decreases to vanishing. With the increasing of charge-to-mass ratio, for example, $\kappa = 0.9$, the absolute value of angular velocity would monotonically decrease. The curves for small black holes corresponding to $\gamma < 1$ look like the capital **U** upside down and thus the absolute value of the angular velocity has the minimum value. For large black holes, the absolute value of the angular velocity on the event horizon monotonically decreases until it is vanishing.

In the next, let's turn to the study of radius for innermost stable circular orbits. We don't bother to list the expression for R since R is the root of a quartic equation. But we have shown the evolution of radius for ISCO and the relative correction to radius of ISCO, $\frac{R_1}{R}$ with respect to γ , respectively, in Fig. 14.

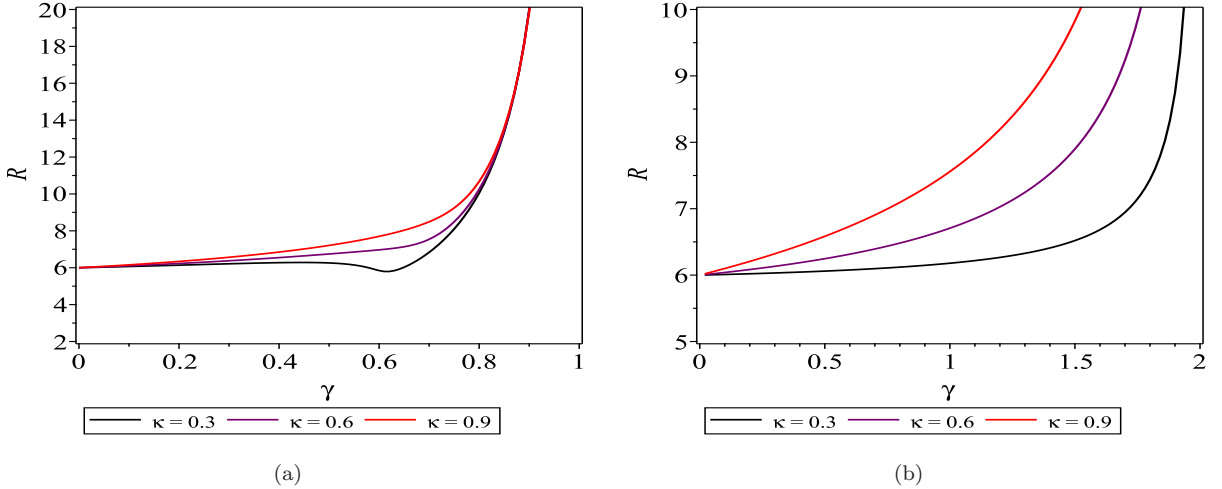


FIG. 14: (a) The radius of ISCO with respect to γ for small black holes. (b) The radius of ISCO with respect to γ for large black holes. The charge-to-mass ratios is set equal to 0.3, 0.6, 0.9.

Fig. 14 shows that for small black holes, the range of γ is constrained in $(0, 1)$ because there doesn't exist stable circular orbits for $\gamma > 1$. On the other hand, for large black holes, the range of γ is constrained in $(0, 2)$. On the whole, the radius of ISCO for both small and large black holes increases with respect to γ from $6M$ corresponding to the Schwarzschild black hole to infinity. But for small black holes and with the smaller charge-to-mass ratio, for example $\kappa = 0.3$, the radius of ISCO can decrease to a minimum radius which is smaller than $6M$.

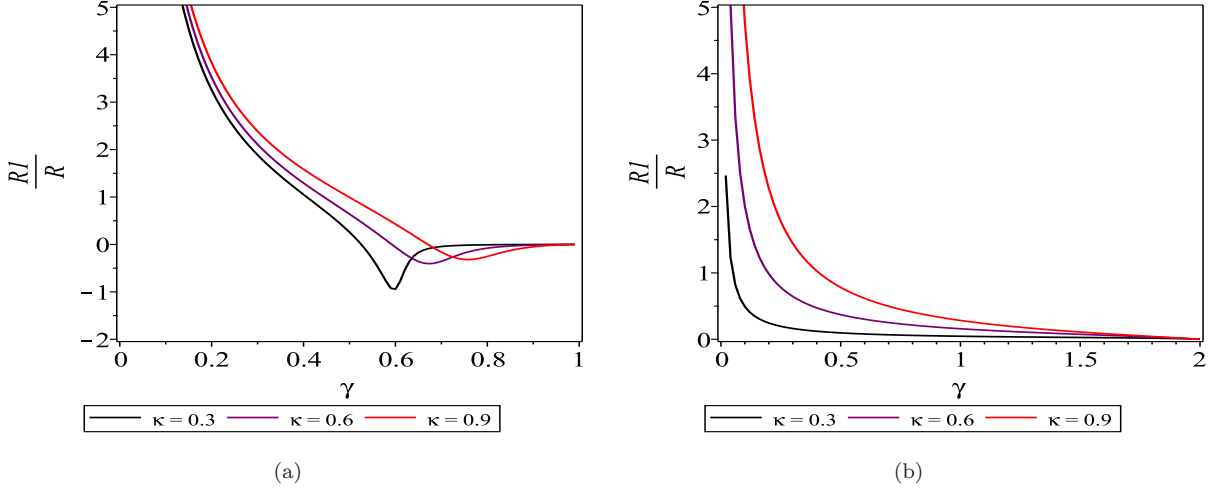


FIG. 15: (a)The relative correction to radius of ISCO with respect to γ for small black holes. (b)The relative correction to radius of ISCO with respect to γ for small black holes. The charge-to-mass ratios is set equal to 0.3, 0.6, 0.9, respectively.

In Fig. 15, we plot the evolution of relative correction R_1/R to the radius of ISCO with respect to γ . From the figure we see, for small black holes, the relative correction firstly decreases to a minimum and then increases to zero.

The relative correction to ISCO for large black holes monotonically decreases to zero and the relative correction becomes larger and larger with the increasing of charge-to-mass ratio, κ .

Finally, let's study the effect of γ on the radiative efficiency η . In Fig. 16 and Fig. 17, we plot the evolution of zeroth order radiative efficiency η_0 and first order radiative efficiency η_1 with respect to γ , respectively. The figure

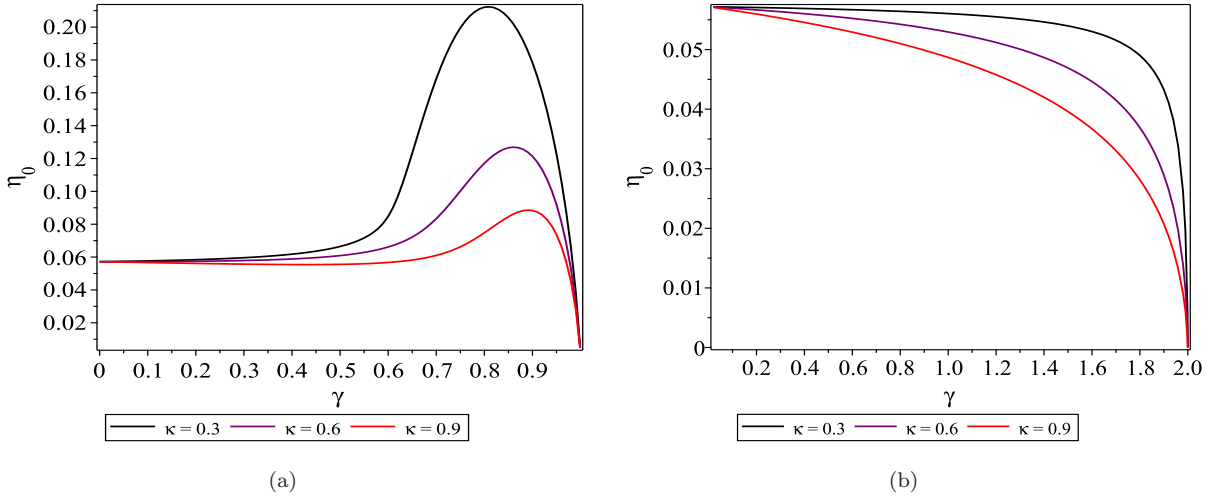


FIG. 16: (a)The zeroth order radiative efficiency η_0 with respect to γ for the small black holes. (b) The zeroth order radiative efficiency η_0 with respect to γ for the large black holes. The charge-to-mass ratios is set equal to 0.3, 0.6, 0.9, respectively.

shows that, for small black holes, both the zeroth order and the first order of efficiency increases at first and then decrease until vanishing. There exists a maximum for the efficiency and the black holes with small mass-to-charge ratio has the larger maximum efficiency. For the large black holes, both the zeroth order and the first order of efficiency (magnitude) monotonically decreases until vanishing.

Taking the zeroth and first order of radiation efficiency into account, we find the total efficiency can vanish for both small black holes and large black holes when γ is small and ϵ is positive as shown in Fig. 18. We remember that the same conclusion has been drawn for normal coupling in section IV.

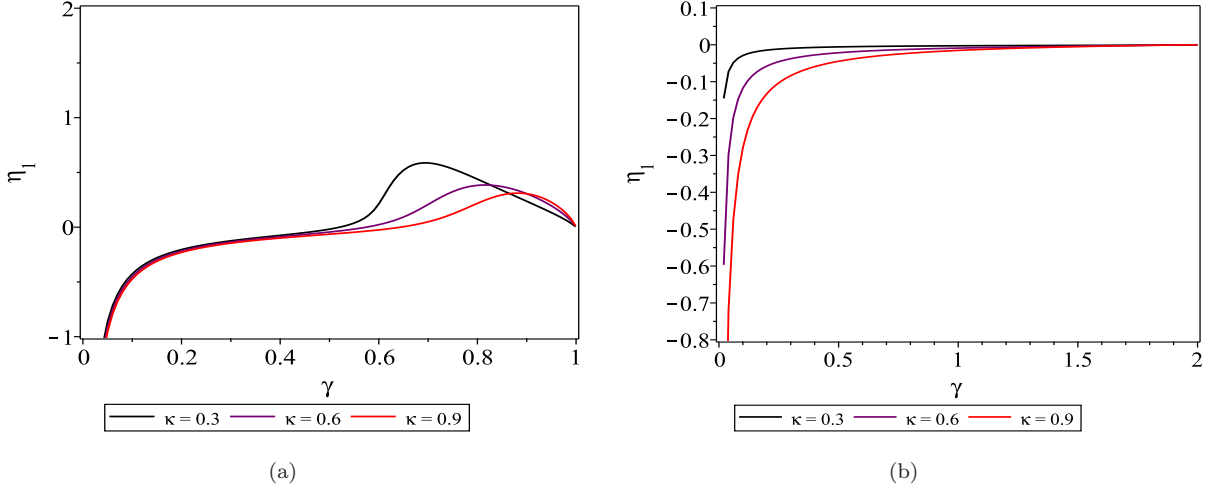


FIG. 17: (a) The first order radiative efficiency η_1 with respect to γ for the small black holes. (b) The first order radiative efficiency η_1 with respect to γ for the large black holes. The charge-to-mass ratios is set equal to 0.3, 0.6, 0.9, respectively.

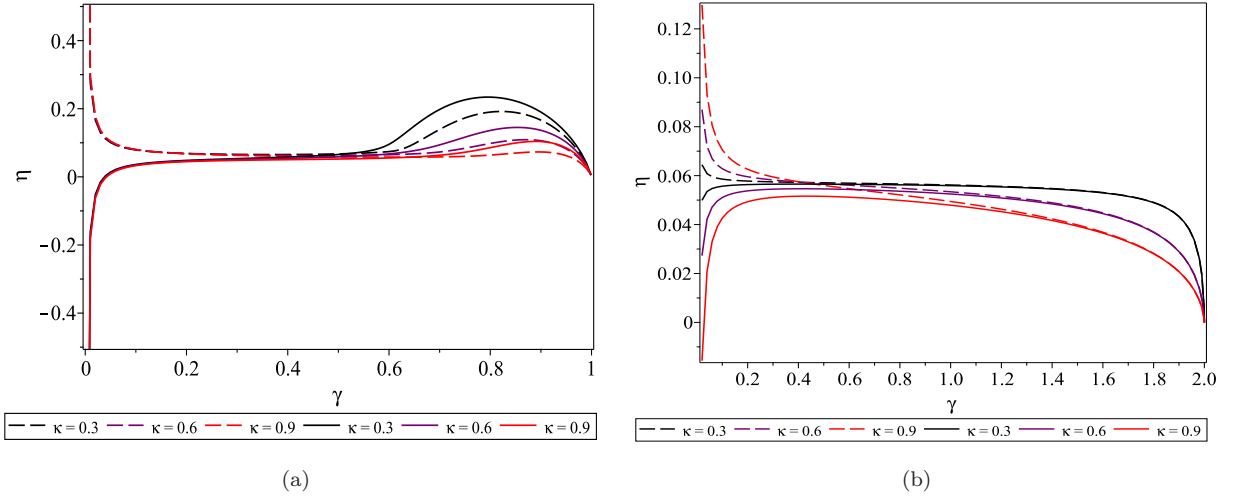


FIG. 18: (a) The efficiency η with respect to γ for the small black hole. (b) The efficiency η with respect to γ for the large black hole. The solid line corresponds to $\epsilon = 0.05$ and dashed line corresponds to $\epsilon = -0.05$. The charge-to-mass ratios is set equal to 0.3, 0.6, 0.9.

VI. SUMMARY

In this paper, we restrict ourselves to action (11) which is the four dimensional case of action (1) and the scala potential is neglected. It is a new Einstein-Maxwell-scalar theory and can be viewed as the combination of various dilaton field with different coupling strength in the Einstein-Maxwell-dilaton frame. We outline the main results as follows.

1. The condition of asymptotically flatness is not sufficient to determine the solution for the slowly rotating black hole. Therefore, in order to specify the constant of integration for any value of β which is later proved to be proportional to angular momentum of the black hole, the regular condition on the outermost event horizon must be imposed.

2. We constrain the range of β by requiring the black hole to be not naked and the coupling between scalar field and Maxwell field $K(\phi)$ to be normal (not phantom). By so doing, we find the range of γ cannot be $[0, 2)$ for some value of β . Then we research on the gyromagnetic ratio of the black hole. For fixed value of b/a and β , the gyromagnetic ratio decreases with the increasing of γ . For fixed value of b/a and γ , the gyromagnetic ratio increases with the

increasing of β . Therefore, the gyromagnetic ratio, 2, of the 4-dimensional Kerr-Newman black hole can be realized by increasing the value of β and γ at the same time.

3. We have investigated the case of $\alpha = 1$ as a specific example. The gyromagnetic ratio with respect to charge-to-mass ratio is studied. We find the gyromagnetic ratio increases with the increasing of β , and decreases with the increasing of $\frac{Q}{M}$. Inspired by this point, the gyromagnetic ratio can be realized again by increasing β and $\frac{Q}{M}$ simultaneously. The dimensionless angular velocity of a locally non-rotating observer on the event horizon is also studied. We find that by increasing $\frac{Q}{M}$ and β , the value of Kerr-Newman black hole, 2, can also be realized.

4. The corrections to the period of circular orbits and the radius of inner most stable circular orbits are also studied. It is found the relative correction decreases with β and increases with $\frac{Q}{M}$. We also studied the radiative efficiency and the related correction in the thin accretion disk model. It's found that for small value of β and negative perturbation parameter, the black hole's ability of capturing the particles become so weak that the accreted matter around it is very dilute. This leads to the conclusion that the radiation cannot be generated due to lacking of enough stress and dynamic friction.

5. We find an exact, slowly rotating black hole solution with phantom Maxwell field. Given a charge-to-mass ratio, there are two black holes solutions which we denote them by small and large black holes, respectively. When $\gamma > 1$, the small black holes have the negative mass. The gyromagnetic ratio is investigated and it is found that the range of γ shrinks with the increasing of $\frac{Q}{M}$ and the signature of gyromagnetic ratio can be positive or negative.

6. The angular velocity for the local non-rotating observer on the event horizon is investigated and it is found that for small black holes, there exists zero point which represents the vanishing of angular velocity. The angular velocity is found to be always negative for both small and large black holes. For small black holes, the angular velocity diverges at $\gamma = 1$ where there doesn't exist small black holes. For large black holes, the absolute angular velocity decreases with the increasing of γ . The differences between corrections to innermost stable circular orbits and the radiative efficiency for small and large black holes are also shown. It is found that the corrections for the large black hole are always monotonous while the turning points are common for both small and large black holes. The negativeness of the correction for small black holes indicates the existence of zero point for the correction. For both small and large black holes, there exists the point where the radiative efficiency is vanishing when the effect of rotation is taken into consideration.

ACKNOWLEDGMENTS

This work is partially supported by the Strategic Priority Research Program "Multi-wavelength Gravitational Wave Universe" of the CAS, Grant No. XDB23040100 and the NSFC under grants 11633004, 11773031.

-
- [1] C. Rovelli, arXiv preprint gr-qc/9803024 (1998).
 - [2] C. Cheung, A. L. Fitzpatrick, J. Kaplan, L. Senatore, and P. Creminelli, *Journal of High Energy Physics* **2008**, 014 (2008).
 - [3] S. Weinberg, *Physical Review D* **77**, 123541 (2008).
 - [4] B. Famaey and S. S. McGaugh, *Living reviews in relativity* **15**, 10 (2012).
 - [5] T. Clifton, P. G. Ferreira, A. Padilla, and C. Skordis, *Physics reports* **513**, 1 (2012).
 - [6] A. Joyce, L. Lombriser, and F. Schmidt, *Annual Review of Nuclear and Particle Science* **66**, 95 (2016).
 - [7] C. Brans and R. H. Dicke, *Physical review* **124**, 925 (1961).
 - [8] J. O'Hanlon, *Physical Review Letters* **29**, 137 (1972).
 - [9] R. Acharya and P. Hogan, *Lettere al Nuovo Cimento* (1971-1985) **6**, 668 (1973).
 - [10] Y. Fujii, *Nature Physical Science* **234**, 5 (1971).
 - [11] Y. Fujii and K.-i. Maeda, *The scalar-tensor theory of gravitation* (Cambridge University Press, 2003).
 - [12] J. Sonner and P. K. Townsend, *Physical Review D* **74**, 103508 (2006).
 - [13] G. W. Gibbons and K.-i. Maeda, *Nuclear Physics B* **298**, 741 (1988).
 - [14] D. Garfinkle, G. T. Horowitz, and A. Strominger, *Physical Review D* **43**, 3140 (1991).
 - [15] R.-G. Cai and Y.-Z. Zhang, *Physical Review D* **54**, 4891 (1996).
 - [16] R.-G. Cai, J.-Y. Ji, and K.-S. Soh, *Physical Review D* **57**, 6547 (1998).
 - [17] H. K. Kunduri and J. Lucietti, *Physics Letters B* **609**, 143 (2005).

- [18] J. Kunz, D. Maison, F. Navarro-Lérida, and J. Viebahn, *Physics Letters B* **639**, 95 (2006).
- [19] Y. Brihaye, E. Radu, and C. Stelea, *Classical and Quantum Gravity* **24**, 4839 (2007).
- [20] A. Sen, *Physical Review Letters* **69**, 1006 (1992).
- [21] K. Hioki and U. Miyamoto, *Physical Review D* **78**, 044007 (2008).
- [22] P. Pradhan, *The European Physical Journal C* **76**, 131 (2016).
- [23] R. Uniyal, H. Nandan, and K. Purohit, *Classical and Quantum Gravity* **35**, 025003 (2017).
- [24] R. Casadio, B. Harms, Y. Leblanc, and P. Cox, *Physical Review D* **55**, 814 (1997).
- [25] J. H. Horne and G. T. Horowitz, *Physical Review D* **46**, 1340 (1992).
- [26] K. Shiraishi, *Physics Letters A* **166**, 298 (1992).
- [27] A. Sheykhi, *Physical Review D* **76**, 124025 (2007).
- [28] A. Sheykhi, M. Allahverdizadeh, Y. Bahrampour, and M. Rahnama, *Physics Letters B* **666**, 82 (2008).
- [29] T. Ghosh and S. SenGupta, *Physical Review D* **76**, 087504 (2007).
- [30] D. Ayzenberg and N. Yunes, *Physical Review D* **90**, 044066 (2014).
- [31] R. R. Caldwell, *Physics Letters B* **545**, 23 (2002).
- [32] B. McInnes, *Journal of High Energy Physics* **2002**, 029 (2002).
- [33] S. Nojiri and S. D. Odintsov, *Physics Letters B* **562**, 147 (2003).
- [34] A. Liddle, *An introduction to modern cosmology* (John Wiley & Sons, 2015).
- [35] A. Melchiorri, L. Mersini, C. J. Ödman, and M. Trodden, *Physical Review D* **68**, 043509 (2003).
- [36] G. Clément, J. C. Fabris, and M. E. Rodrigues, *Physical Review D* **79**, 064021 (2009).
- [37] C. J. Gao and S. N. Zhang, *Physical Review D* **70**, 124019 (2004).
- [38] C. J. Gao and S. N. Zhang, *Physics Letters B* **605**, 185 (2005).
- [39] S. Yu, J. Qiu, and C. Gao, arXiv preprint arXiv:2005.14476 (2020).
- [40] J. Qiu and C. Gao, *Universe* **6**, 148 (2020).
- [41] B. Turimov, J. Rayimbaev, A. Abdujabbarov, B. Ahmedov, and Z. Stuchlík, *Physical Review D* **102**, 064052 (2020).
- [42] E. Barausse, T. P. Sotiriou, and I. Vega, *Physical Review D* **93**, 044044 (2016).
- [43] J. D. Brown and J. W. York Jr, *Physical Review D* **47**, 1407 (1993).
- [44] E.ourgoulhon, *3+ 1 formalism in general relativity: bases of numerical relativity*, Vol. 846 (Springer Science & Business Media, 2012).
- [45] M. Shibata and M. Sasaki, *Physical Review D* **58**, 104011 (1998).